Supplementary Information for

Uncertainties in Riverine and Coastal Flood Impacts under Climate Change

Shuyi Wang, Mohammad Reza Najafi, Alex J. Cannon and Amir Ali Khan

Supplementary Table 1. Roughness value (manning's n) for different land cover types

Land Cover Type	Roughness (Manning's n)
Barren lands	0.03
Forest	0.13
Grassland	0.04
Shrubland	0.12
Lichen-moss	0.03
Urban	0.1
Water	0.04
Wetland	0.1

Supplementary Table 2. Characteristics of the selected GCMs

GCMS	MODELING CENTER	RESOLUTION (ATMOSPHERE)	AVAILABLE DATA
ACCESS1.0	Commonwealth Scientific and Industrial Research Organization and Bureau of Meteorology	1.25 x 1.875 degree	1950-2005 2006-2100
CANESM2	Canadian Centre for Climate Modelling and Analysis	2.8 x 2.8 degree	1850-2005 2006-2100

CSIRO-MK3.6.0	Australia's national science agency Atmospheric Research	1.86 x 1.875 degree	1950-2005 2006-2300
GFDL-CM3	Geophysical Fluid Dynamics Laboratory	2 x 2.5 degree	1860-2005 2006-2100
GFDL-ESM2G	Geophysical Fluid Dynamics Laboratory	2 x 2.5 degree	1860-2005 2006-2100
HADGEM2-AO	Institute of Meteorological Research/Korea Meteorological Administration	1.25 x 1.875 degree	1860-2005 2006-2100
HADGEM2-CC	UK Met Office Hadley Centre Carbon Cycle Model	1.25 x 1.875 degree	1950-2005 2006-2100
HADGEM2-ES	UK Met Office Hadley Centre Carbon Cycle Model	1.25 x 1.875 degree	1860-2005 2006-2100
MPI-ESM-LR	Max Planck Institute for Meteorology	1.86 x 1.875 degree	1979-2005 2006-2300

Supplementary Table 3. List of satellite images including the reference images and the flood image

Satellite	Image type	Image Date	Resolution (m)	Mode	Polarization

Sentinel-1A	Reference	20171208	10	IW	HH
		20171220			
		20180101			
		20180125			
		20181215			
		20181227			
		20181204			
		20190108			
		20190120			
	Flood	20180114			

Supplementary Table 4. List of scenarios and the simulations

Projected IDF curves	**WRF-IDF curve**	**GCM-IDF curve**
Future period	2050s (2041-2070) & 2080s (2071-2100)	
Return period	25-year and 100-year flood events	
RCP	RCPs 4.5 & 8.5	
GCMs	ACCESS1.0, HadGEM2-CC, HadGEM2-ES, GFDL-CM3, MPI-ESM-LR, HadGEM-AO, CSIRO-Mk3.6.0, GFDL-ESM2G, and CanESM2 (total 9)	HadGEM2-ES, GFDL-CM3, HadGEM-AO, CSIRO-Mk3.6.0, GFDL-ESM2G, and CanESM2 (total 6)
Design storms	SCS method Huff method ABM method (2 ways)	SCS method Huff method ABM method
Total No. hyetographs	288	144

Peak rainfall values for all future scenarios by CanESM2 are detailed in Tables S5&S6. The hyetographs generated by WRF-IDF curves are projected to have a higher peak precipitation

intensity based on RCP 8.5 compared to the RCP 4.5 hyetographs in both future periods. However, the RCP 8.5 peak rainfall generated based on GCM-IDF curves is estimated to be lower than that in RCP 4.5 hyetographs for the 2050s period. RCP 4.5 is an intermediate emission scenario indicating that carbon emissions will decrease after reaching the peak, while RCP 8.5, as the worst-case scenario of climate change models, assumes that the carbon emissions will continue to rise in the future. According to the tables, the magnitude of rainfall in the RCP 8.5 scenario is larger compared to the RCP4.5 scenario in most cases. However, design storms by GCM-IDF curves give a lower estimation for the future period of the 2050s. From RCP 4.5 to RCP 8.5, and from 25-year event to 100 year-event, the trends of hyetographs by WRF-IDF curves remain consistent for all periods and design storm methods. The incoherence GCM-IDF generated hyetographs may be associated with the uncertainty in the projected IDF curves based on GCM precipitation estimations. Comparison between the three design storm methods shows that there is more considerable variation between rainfall peaks associated with higher return-level events in the 2080s, compared to those in the 2050s. Therefore, the hyetographs for 100-year flood events in the 2080s have the largest uncertainties. The duration of peak rainfall can further affect the rainfall-runoff simulations in addition to the differences in peak rainfall values.

Supplementary Table 5. Peak Rainfall (mm) values corresponding to WRF- and GCM-IDF curves based on CanESM2 simulations in the 2050s

SCS method	WRF-IDF curves		GCM-IDF curves	
Return period	25yr	100yr	25yr	100yr
RCP 4.5	30.16	37.10	33.32	50.45
RCP 8.5	31.44	38.73	32.48	44.88
DIFF between RCPs	1.28	1.62	***-0.84***	***-5.56***

Huff method	WRF-IDF curves		GCM-IDF curves	
Return period	25yr	100yr	25yr	100yr
RCP 4.5	13.17	16.20	14.55	22.03
RCP 8.5	13.73	16.91	14.18	19.60
DIFF between RCPs	0.56	0.71	***-0.37***	***-2.43***

ABM method	WRF-IDF curves				GCM-IDF curves	
	ABM1		ABM2			
Return period	25yr	100yr	25yr	100yr	25yr	100yr
RCP 4.5	32.90	40.66	36.63	45.21	39.17	57.85
RCP 8.5	34.30	42.44	38.80	47.94	38.17	52.01
DIFF between RCPs	1.40	1.78	2.18	2.73	***-0.99***	***-5.84***

Supplementary Table 6. Peak Rainfall (mm) values corresponding to WRF- and GCM-IDF curves based on CanESM2 simulations in the 2080s

SCS method	WRF-IDF curves		GCM-IDF curves	
Return period	25yr	100yr	25yr	100yr
RCP 4.5	31.33	38.59	29.66	45.78
RCP 8.5	36.09	44.62	36.90	49.61
DIFF between RCPs	4.77	6.04	7.25	3.83

Huff method	WRF-IDF curves		GCM-IDF curves	
Return period	25yr	100yr	25yr	100yr
RCP 4.5	13.68	16.85	12.95	19.99
RCP 8.5	15.76	19.49	16.12	21.66
DIFF between RCPs	2.08	2.64	3.17	1.67

ABM method	WRF-IDF curves				GCM-IDF curves	
Return period	25yr-1	100yr-1	25yr-2	100yr-2	25yr	100yr
RCP 4.5	34.17	38.61	42.29	47.70	35.06	52.43
RCP 8.5	39.38	46.71	48.91	57.85	42.93	57.60

DIFF between RCPs	5.20	8.09	6.62	10.14	7.87	5.16

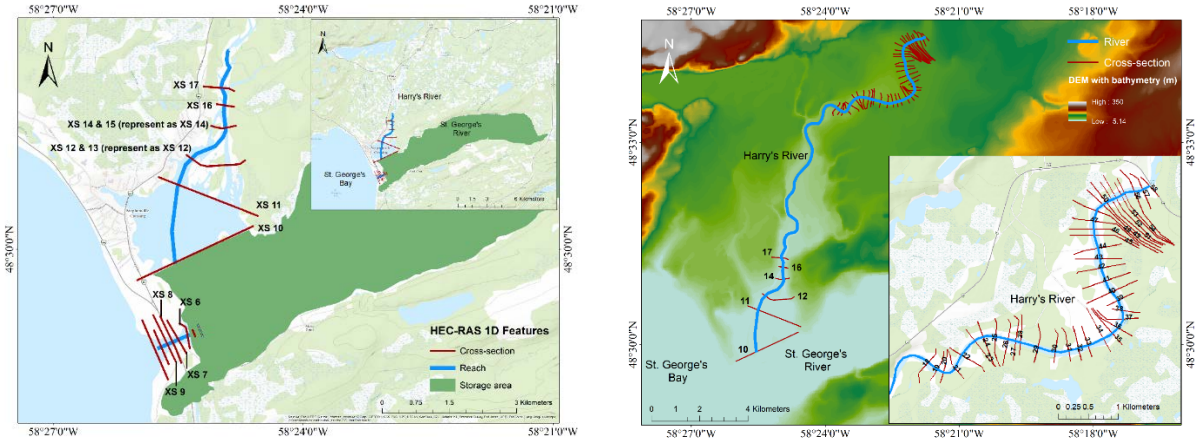

(a) (b)

Supplementary Figure 1. A) Survey cross sections in the HEC-RAS model, b) Additional surveyed cross-sections (red line) with bathymetry-fused DEM

Sentinel-1 satellite does not have any image until 2015 for Stephenville Crossing. According to the flow gauge records, there was potential flooding in January 2018. Therefore, we analyze the associated Sentinel-1 images on 14th January 2018. The comparison between the maximum inundation area of HEC-RAS 2D simulation and Sentinel-1 flood map is shown in Figure 4.9. According to the sentinel-1 image, the upstream part of Harry's River is not flooded, however HEC-RAS 2D shows inundation. The small pixels in the inland area are possible noise from the sentinel-1 image.

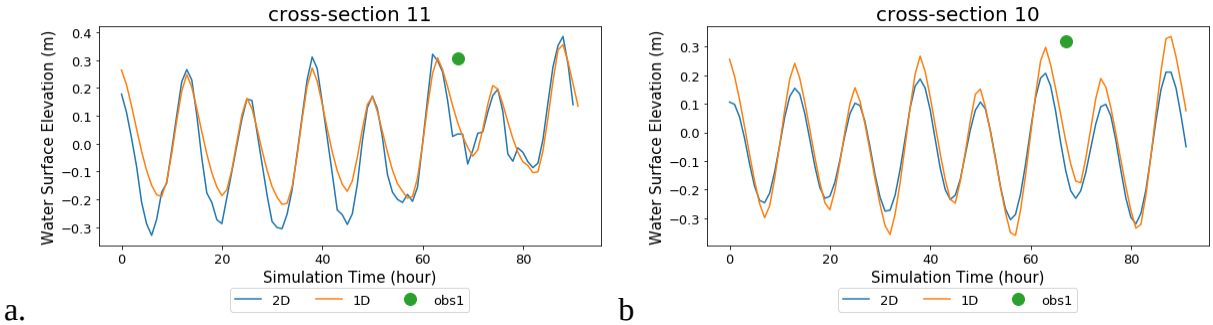

Supplementary Figure 2. HEC-RAS 1D & 2D model evaluation for November 3rd at 8pm November 7th, 2010 at 4pm. Orange represents 1D HEC-RAS results, blue represents 2D HEC-RAS results; obs represents the measurements at 4pm, November 6, 2010

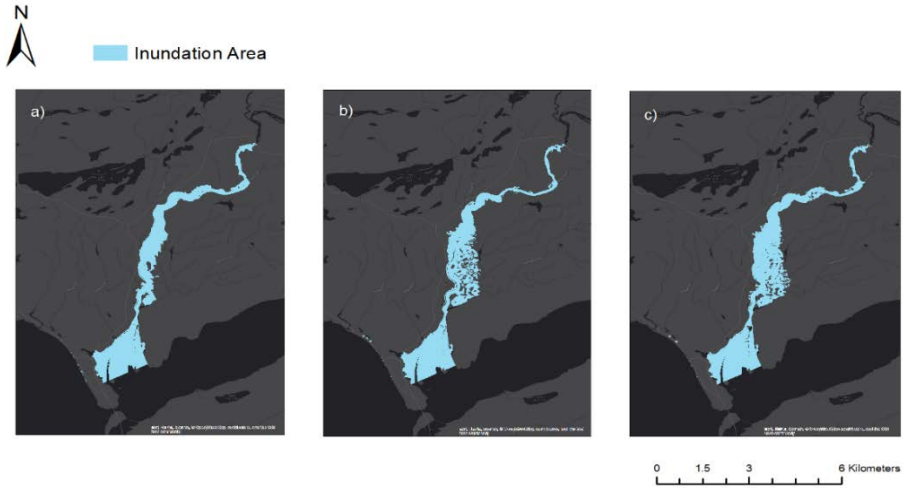

Supplementary Figure 3. Comparison between 2D simulated flood inundation extents based on different roughness values for channel and floodplain: a) 0.033 and 0.05; b) 0.045 and 0.05; c) 0.033 and 0.08

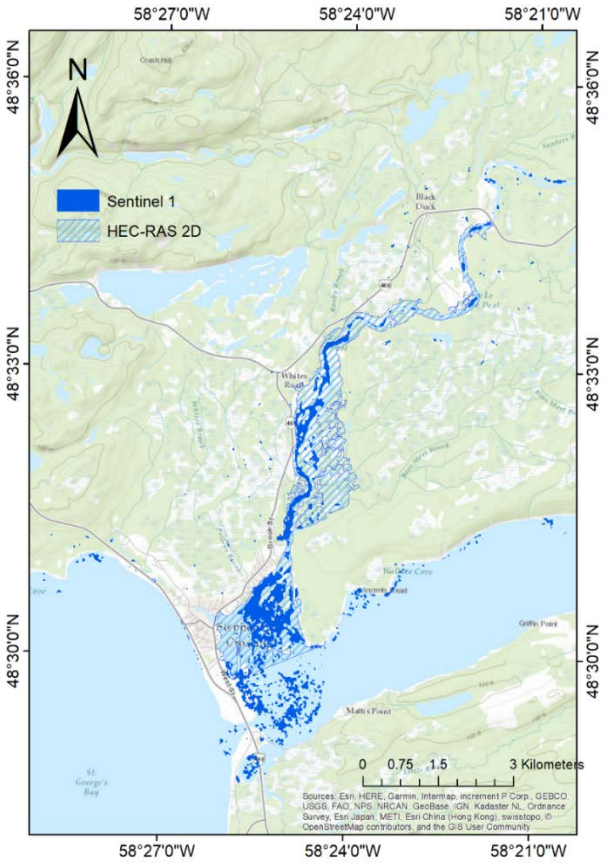

Supplementary Figure 4. The detected flood inundated area based on Sentinel-1 imagery (Jan. 14th, 2018) compared with HEC-RAS 2D model simulations

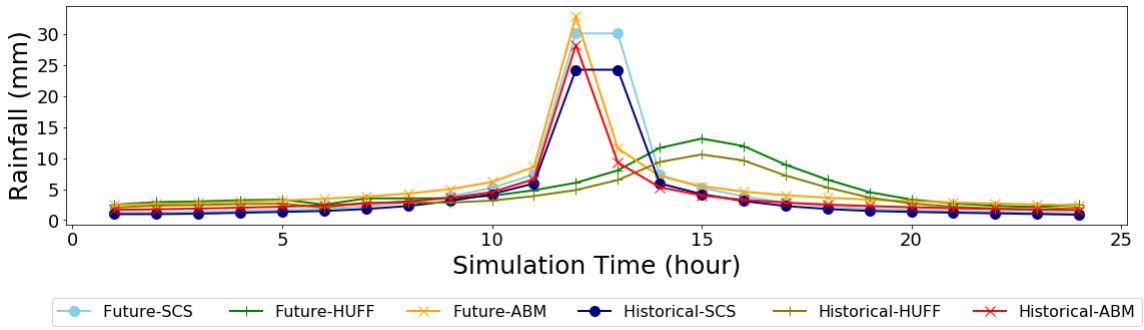

Supplementary Figure 5. Hyetographs corresponding to a 25-year rainfall event generated by three design methods for the historical and future (2050s; RCP 4.5) periods

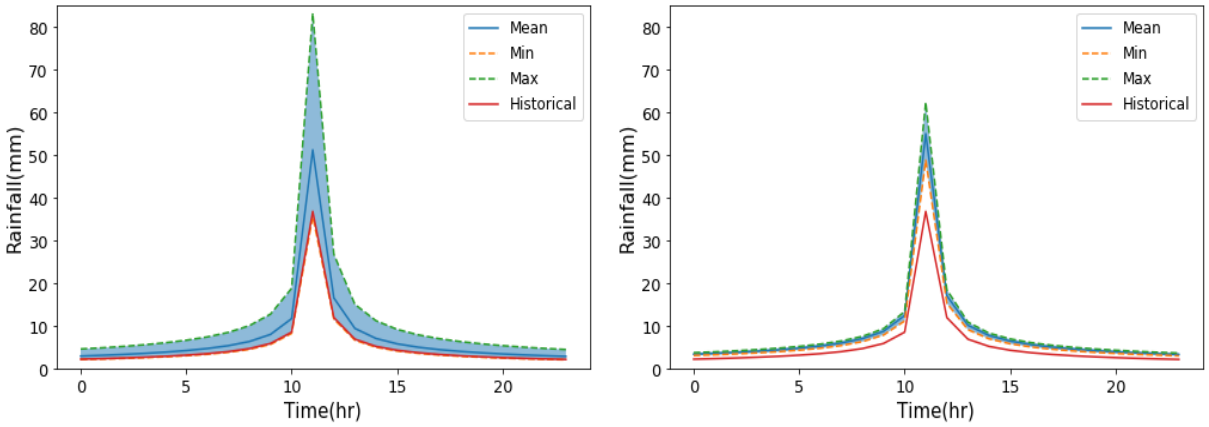

a. b.

Supplementary Figure 6. Similar to Figure 5 but for 100-year event and future period of 2080s corresponding to RCP 8.5 emission scenario a) GCM-IDF (ABM) and b) WRF-IDF (ABM-2)

ABM Method

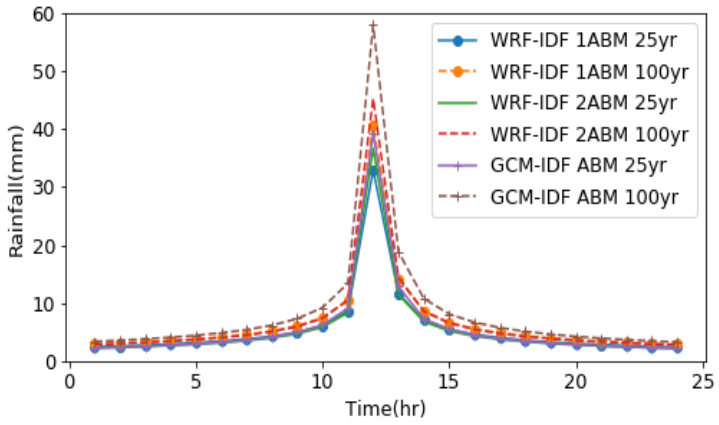

SCS Method

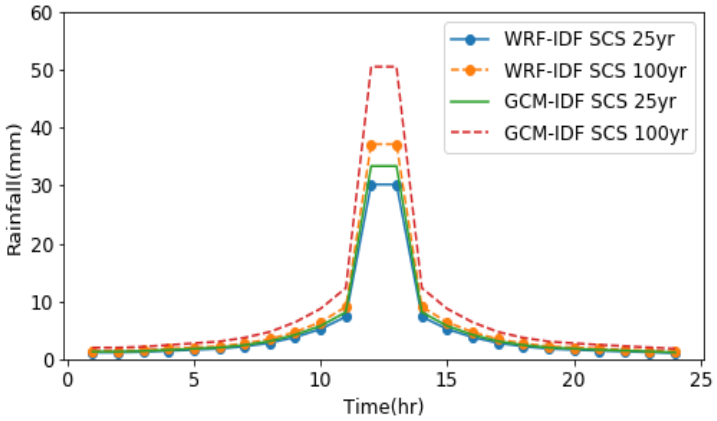

HUFF Method

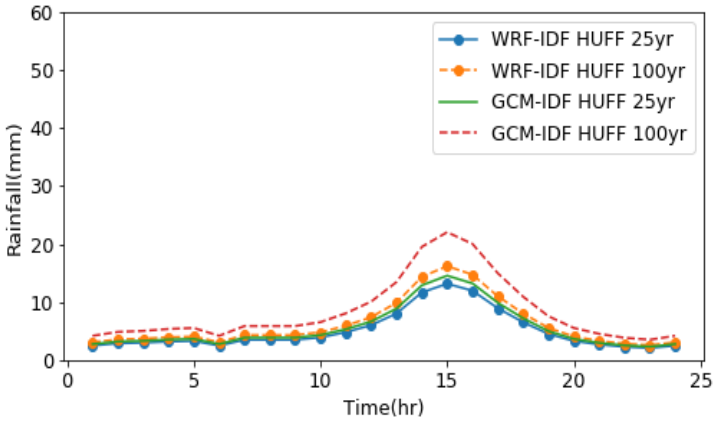

Supplementary Figure 7. Rainfall hyetographs corresponding to CanESM2 simulations for 2050s under RCP4.5

ABM Method

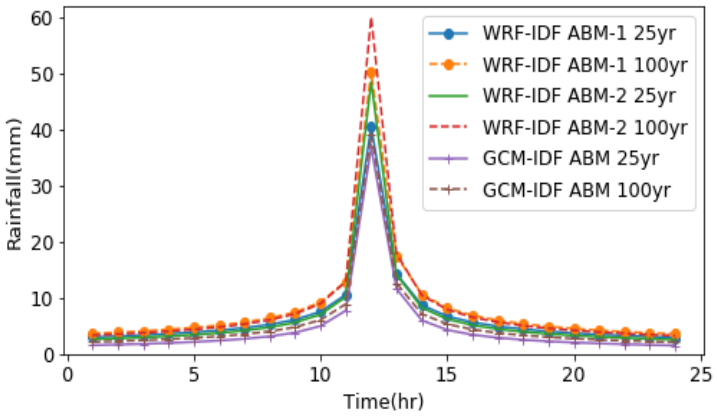

SCS Method

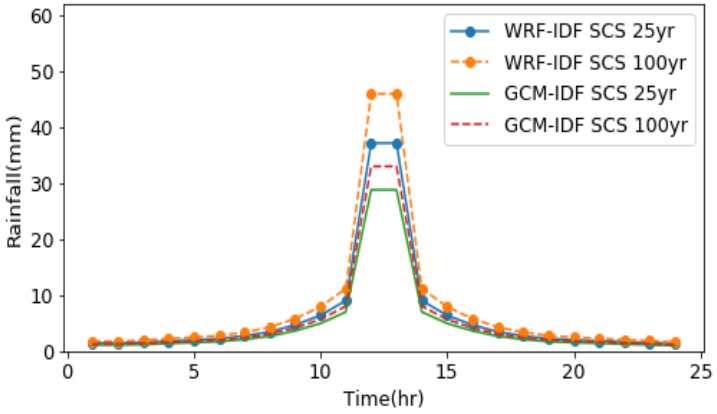

HUFF Method

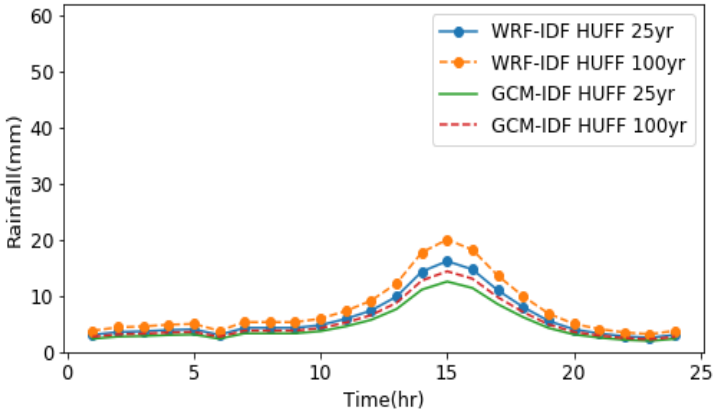

Supplementary Figure 8. Rainfall hyetographs corresponding to HadGEM-AO (AO) simulations for 2080s under RCP8.5

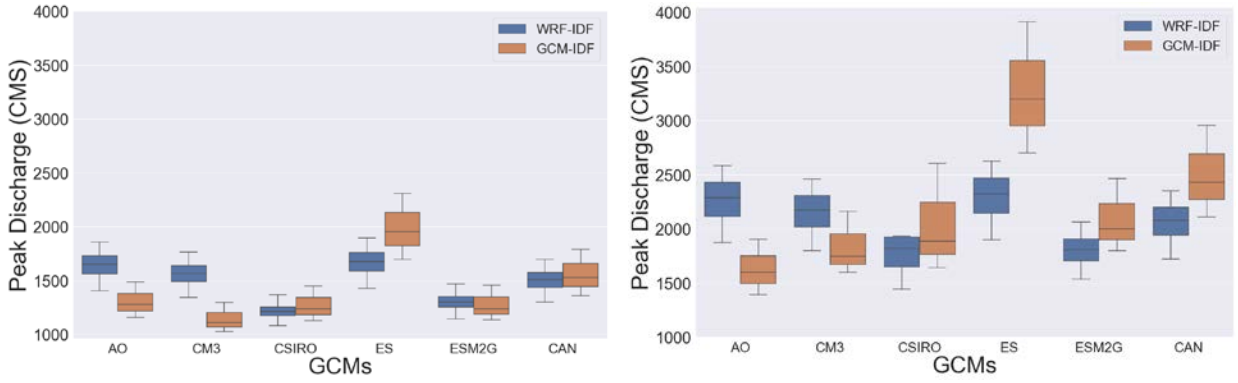

(a) (b)

Supplementary Figure 9. Simulated peak discharge rates corresponding to WRF- and GCM-IDFs for a) 25-yr event and b) 100-yr event. Both simulations correspond to 2050s (2041-2070) under RCP 8.5. emission scenario. The participating GCMs include: HadGEM-AO (AO), GFDL-CM3 (CM3), CSIRO-Mk3.6.0 (CSIRO), HadGEM2-ES (ES), GFDL-ESM2G (ESM2G), and CanESM2 (CAN)

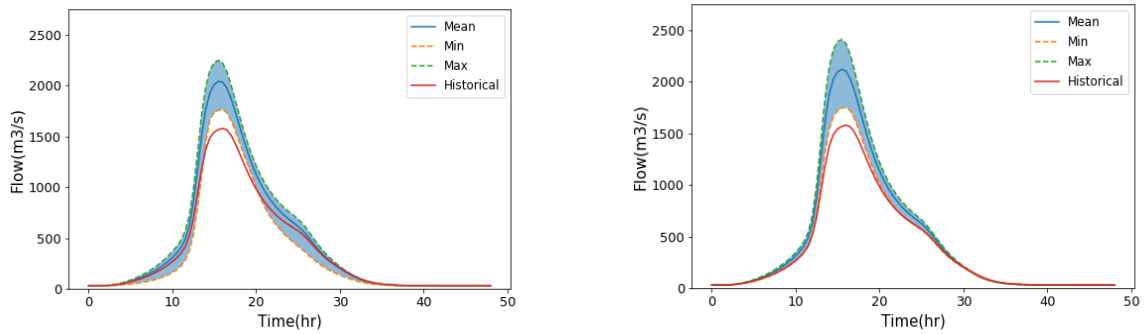

(a) (b)

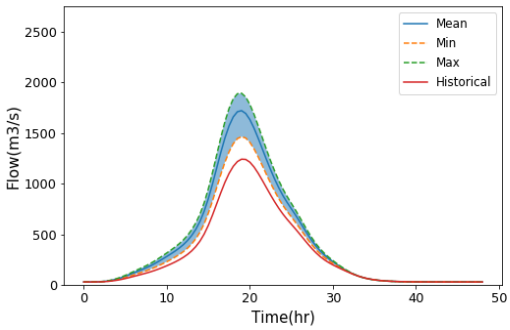

(c)

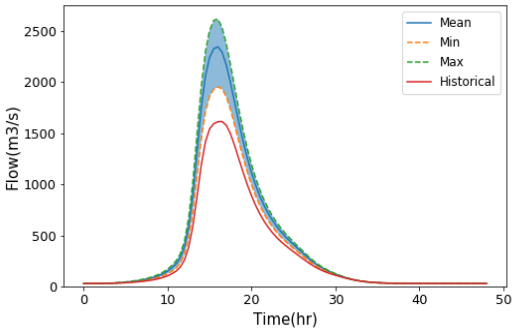

(d)

Supplementary Figure 10. Projected HEC-HMS hydrographs corresponding to the 100-year rainfall event for the historical and future (2050s; RCP8.5) conditions. The results correspond to the WRF-IDF curves based on a. ABM1, b. ABM2, c. Huff, d. SCS design storm methods

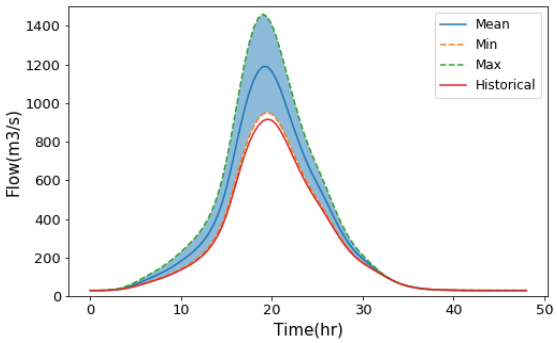

(a)

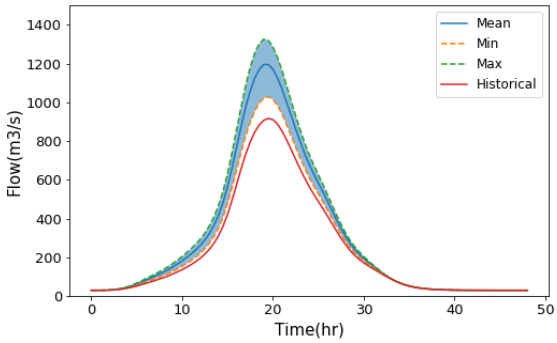

(b)

Supplementary Figure 11. Flow hydrographs at the gauge of Harry's River below Highway Bridge (see location in Figure 1) for a 25-year event corresponding to the historical and future (2050s, RCP4.5) periods. Hyetographs are generated based on the HUFF method and a) GCM-IDFs b) WRF-IDFs

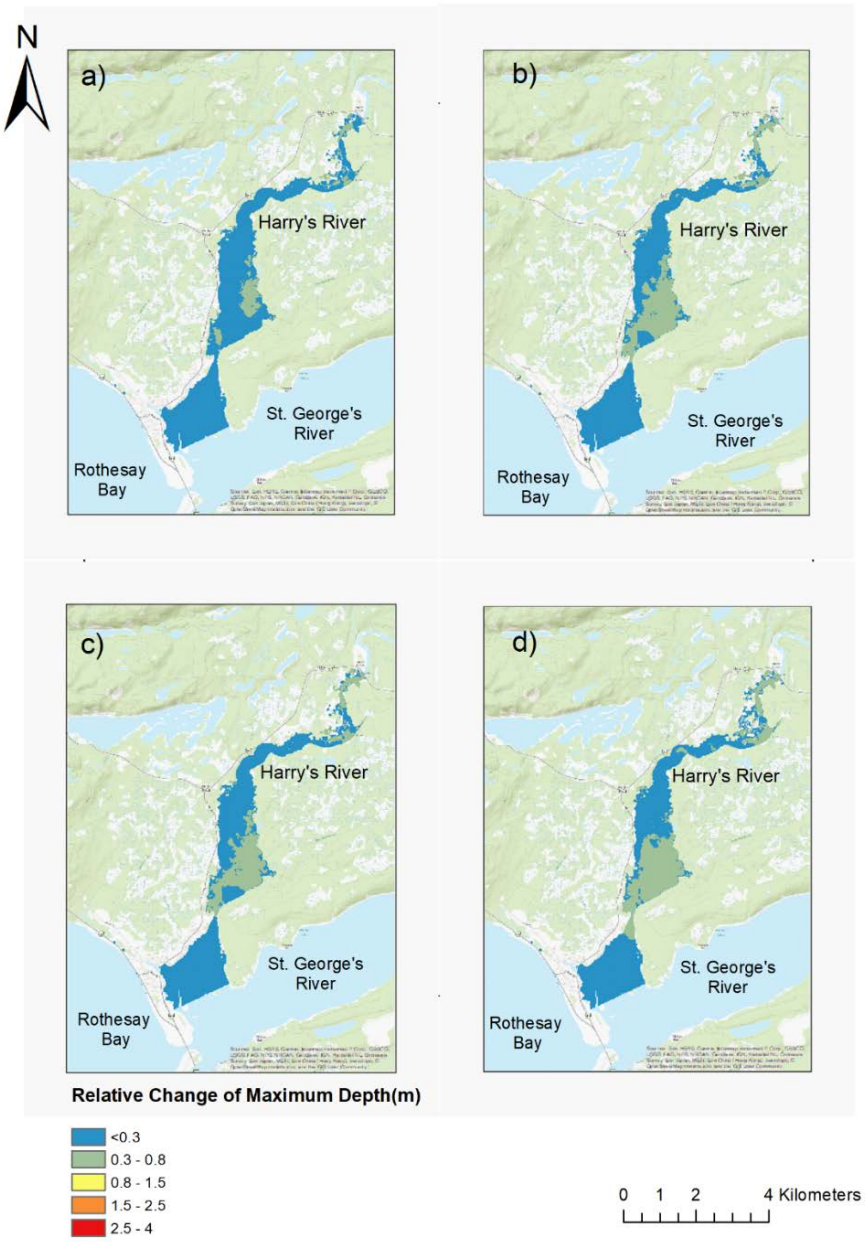

Supplementary Figure 12. Projected changes in maximum flood depths corresponding to a 25-year event between future (2050s) and historical periods; a) GCM-IDF & RCP 4.5, b) WRF-IDF & RCP 4.5, c) GCM-IDF & RCP 8.5, d) WRF-IDF & RCP 8.5

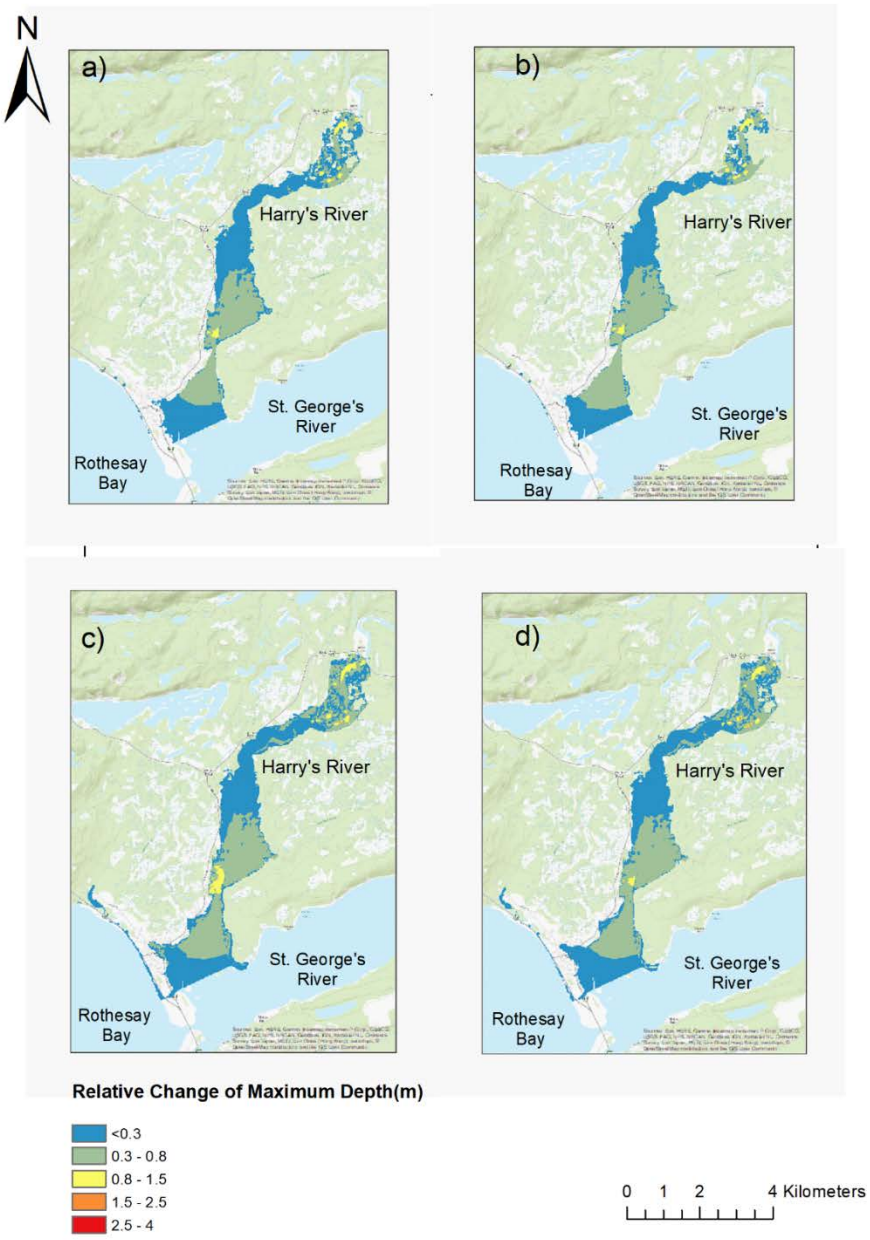

Supplementary Figure 13. Projected changes in maximum flood depths corresponding to a 100-year event between future (2050s) and historical periods; a) GCM-IDF & RCP 4.5, b) WRF-IDF & RCP 4.5, c) GCM-IDF & RCP 8.5, d) WRF-IDF & RCP 8.5

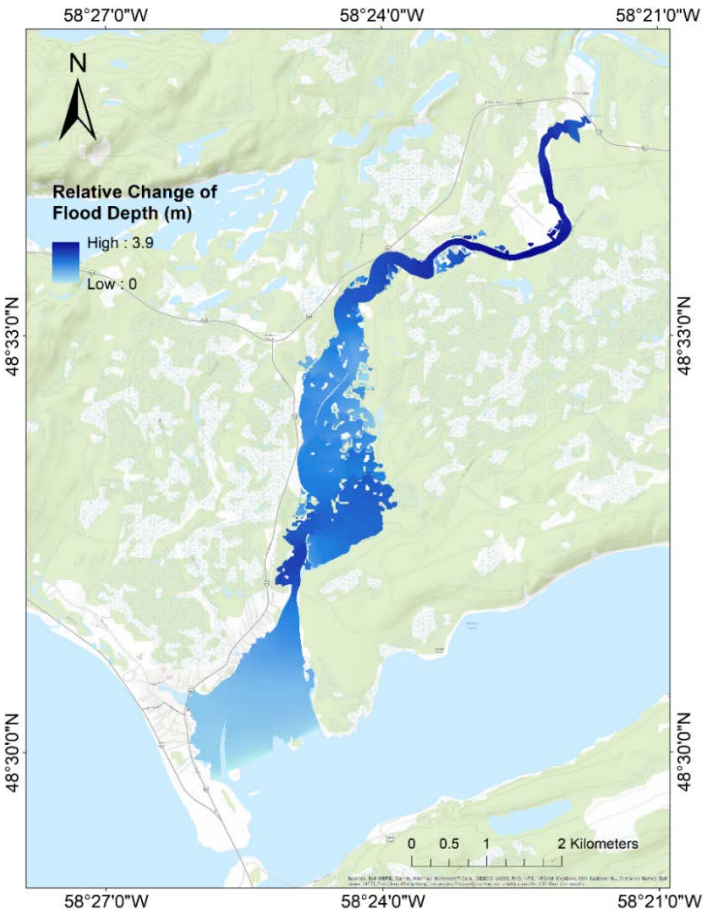

Supplementary Figure 14. Projected changes in 25-year flood inundation corresponding to RCP 4.5 in 2050s compared to the historical condition (based on the SCS design storm method)